ACS APPLIED MATERIALS & INTERFACES

Research Article

www.acsami.org

Layered Double Hydroxide Functionalized Textile for Effective Oil/Water Separation and Selective Oil Adsorption

Xiaojuan Liu, Lei Ge, Wei Li, Xiuzhong Wang, and Feng Li*

College of Chemistry and Pharmaceutical Sciences, Qingdao Agricultural University, Qingdao 266109, People's Republic of China

Supporting Information

ABSTRACT: The removal of oil and organic pollutants from water is highly desired due to frequent oil spill accidents, as well as the increase of industrial oily wastewater. Here, superhydrophobic and superoleophilic textile has been successfully prepared for the application of effective oil/water separation and selective oil adsorption. This textile was fabricated by functionalizing the commercial textile with layered double hydroxide (LDH) microcrystals and low surface energy molecules. The LDH microcrystals were immobilized on the microfibers of the textile through an in situ growth method, and they formed a nestlike microstructure. The combination of the hierarchical structure and the low surface energy molecules made the textile superhydrophobic and superoleophilic. Further experiments demonstrated that the as-prepared textile not only can be applied as effective membrane materials for the separation of oil and water mixtures with high separation efficiency (>97%), but also can be used as a bag for the selective oil adsorption from water. Thus, such superhydrophobic and superoleophilic textile is a very promising material for the application of oil spill cleanup and industrial oily wastewater treatment.

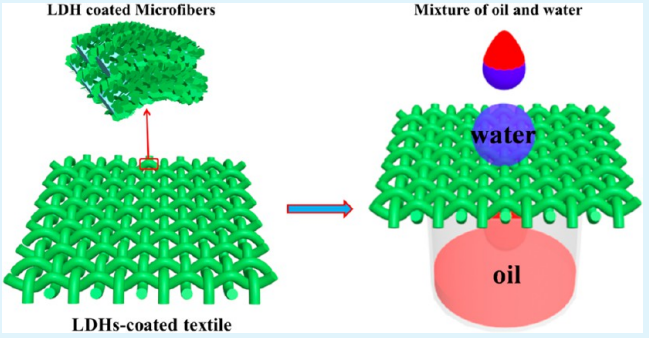

KEYWORDS: *layered double hydroxide, oil/water separation, oil adsorption, superhydrophobic, superoleophilic*

1. INTRODUCTION

With the development of industry and social economy, oil spillage and industrial discharge of organic solvents become more and more serious, which have caused severe environmental and ecological damage.[1,2] Last year, the oil pipeline blast in Qingdao resulted in a large amount of oil spills into ocean that greatly harmed the coastline and near-shore water, creating a disaster for marine animals and organisms. After seeing the great damages of oil spillage, researchers are motivated to design and fabricate functional membrane materials and adsorbents for dealing with oil spills. To achieve the goal of removing oil from water, such membrane materials and adsorbents should be superhydrophobic and superoleophilic.[3] According to the Wenzel model and the Cassie−Baxter model,[4,5] the introduction of a proper rough surface microstructure could make a flat hydrophobic surface more hydrophobic or even superhydrophobic due to the introduction of an air cushion beneath the water droplet, whereas a flat oleophilic surface becomes more oleophilic or even superoleophilic because of the capillary effect.[6,7] Thus, introducing proper rough surface topography on the desired substrates provides a useful route for the preparation of superhydrophobic and superoleophilic materials.[8−11] The rough surface can be constructed by immobilizing nanomaterials on the desired substrate.[12−15] Although great advances have been achieved in the fabrication of nanomaterials,[16,17] it remains a challenge to generate large-scale functional coatings from nanomaterials by simple processes.

Recently, layered double hydroxides (LDH), also known as hydrotalcite-like materials, have received considerable attention due to their interesting properties in compositional flexibility and anion exchangeability.[18,19] These materials can be described by the general formula $[M^{2+}_{1-x}M^{3+}_{x}(OH)_2][A^{n-}_{x/n}]\cdot mH_2O$, where the cations M^{2+} and M^{3+} occupy the octahedral holes in a brucite-like layer and the anion A^{n-} is located in the hydrated interlayer galleries.[20,21] The diversity of the chemical compositions of brucite-like host layers and interlayer anions enables these materials with a wide variety of properties, which make them promising inorganic building blocks toward the generation of films and coatings for applications in many fields such as catalysis, separation, purification, antireflection, biomedicine, etc.[22−30] Furthermore, incorporation of organic anions in LDH films has been demonstrated to endow LDH films with hydrophobic surface properties and widen their applications.[31−34] For example, Vance et al. have synthesized organo-LDH and evaluated their ability to absorb the anionic surfactant.[32] Duan et al. reported that the intercalation of laurate anions by ion exchange with ZnAl-LDH-NO_3^- film precursors on a porous anodic alumina/aluminum (PAO/Al)

Received: October 19, 2014
Accepted: December 9, 2014
Published: December 9, 2014

Scheme 1. Illustration of the Modification of Commercial Textile with LDH and Its Application for Oil/Water Separation

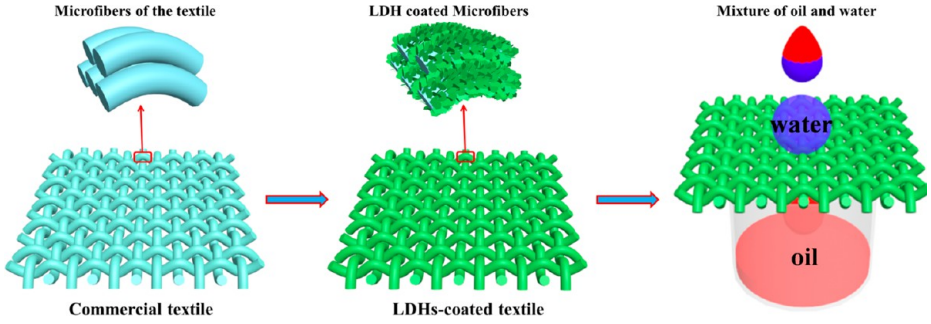

substrate leads to a hierarchical micro-/nanostructured superhydrophobic film, which provides a very effective corrosion-resistant coating for the underlying aluminum.[33] Pramanik et al. have demonstrated the preparation of cone-shaped superhydrophobic and oleophilic CaAl-LDH intercalated with dodecyl sulfate anions and their application in mopping and regeneration of oil−water mixtures.[34]

Before the application of LDH films, it is essential to organize LDH microcrystals into large uniformly aligned LDH arrays or films on the desired substrates. Up to now, various approaches have been employed for the preparation of functional LDH films, such as layer-by-layer self-assembly, solvent mixing, dip-coating, spin-coating, and screen-printing.[35−38] The films produced by the above methods usually have 2D sheet-like structures with face-to-face stacking of the LDH platelets. However, these films have been suggested to have much weaker adhesion between the LDH crystallites than in the films fabricated by in situ growth method, which have a preferred orientation with the *c*-axis perpendicular to the substrate surface.[39,40] Therefore, intensive studies have been focused on the direct growth of oriented LDH microcrystals on different kinds of substrates.[41−46] For instance, MgAl-LDH films can be grown on the surface of anodic aluminum oxide (AAO)/aluminum substrate by dipping the substrate in a mixed reaction solution containing $Mg(NO_3)_2$.[44] NiAl-LDH and ZnAl-LDH films can be grown on porous anodic alumina/aluminum (PAO/Al) substrate by vertically suspending the PAO/Al substrate in a special solution.[45] Alternatively, ZnAl-LDH and CuAl-LDH films can be directly grown on Zn foil and Cu foil, respectively, by immersing the substrates into an alkaline solution.[46] However, in the above processes, qualified substrates should be able to react with the solution and provide cations to form the LDH films on the surfaces of the substrates, which limited the species of the substrate materials and the applications of the functional films. Therefore, it is desirable for the in situ growth of oriented LDH films on inert substrates. In this respect, some positive results have been achieved.[47−50] For example, Duan and co-workers have reported the in situ growth of LDH on some inert substrates, such as glass, paper, polystyrene sheets, and so on.[47−49] Uan et al. have developed a metal salt-free method for directly growing oriented LiAl-LDH films on substrates of grass, silicon wafer, carbon cloth, etc.[50] However, despite the positive results achieved by many research groups, further exploration is still in urgent need, especially for the practical applications of LDH coated substrates. Apart from the LDH coating, the properties of the substrates are equally important for their applications, due to the effect of substrates on the practical applications. For oil/water separation and oil adsorption, textile is considered as one of the most attractive materials and has been widely studied after the 2010 oil spill in the Gulf of Mexico, due to its excellent properties such as flexibility, low price and density, high adsorption capability, as well as high mechanical stability under harsh practical conditions.[10−14] Nevertheless, commercial textile usually can adsorb oil and water at the same time. Although some investigations of superhydrophobic textiles for oil adsorption have been performed,[10−14] there is no information about the in situ growing oriented LDH microcrystals on the surface of textile for oil removal.

With this in mind, herein, superhydrophobic and superoleophilic textile has been fabricated by direct in situ growth of oriented LDH microcrystals on the surface of commercial textile under hydrothermal condition. The simple and inexpensive hydrothermal process shows high flexibility in terms of controlling the structure and morphology of the resulting inorganic materials, which allows us to fabricate high-quality nanoporous LDH coatings on the surface of textile.[51] The LDH coatings have peculiar micro-/nanostructure with nanosheet LDH microcrystals aligned vertically on the surface of textile. As a result, the LDH coated textile exhibits superhydrophobicity after simple modification with surfactant. Additionally, combining superhydrophobicity, superoleophilicity with the excellent properties of textile makes it an excellent material for oil/water separation and selective oil adsorption (Scheme 1).

2. EXPERIMENTAL SECTION

Materials. All chemical regents and solvents were obtained from commercial suppliers and used without further purification. Magnesium nitrate hexahydrate ($Mg(NO_3)_2·6H_2O$), aluminum nitrate nonahydrate ($Al(NO_3)_3·9H_2O$), and sodium hydroxide (NaOH) were obtained from Beijing Chemical Reagent Co. Oil red O, sodium laurate, and methylene blue were purchased from Aladdin. Commercial polyester and cotton textiles were cleaned with 0.2 M NaOH aqueous solution. Deionized water (resistance >18.2 MΩ cm) was used in all reactions.

Fabrication of LDH Coatings. The magnesium−aluminum LDH (MgAl-LDH) coatings on the surface of textile were prepared by the following steps. First, the LDH precursors were synthesized by a coprecipitation process similar to that described previously.[30] Briefly, 1.026 g of $Mg(NO_3)_2·6H_2O$ (4.0 mmol) and 0.7526 g of $Al(NO_3)_3·9H_2O$ (2.0 mmol) were codissolved into 20 mL of water. The mixed aqueous solution then was added quickly into 80 mL of NaOH aqueous solution (0.72 g, 18 mmol) under vigorous stirring. The reaction solution was continuously stirred for another 30 min. The precipitates were isolated by centrifuging and washed with deionized water twice, and then redispersed in deionized water to obtain a 40 mL suspension. Subsequently, the resulting suspension was transferred to a 50 mL Teflon-lined autoclave. The commercial textile was immersed into the suspension, and the mixture was then hydrothermally treated at 100 °C for 24 h. The resultant LDH coated textile was washed with

dx.doi.org/10.1021/am507238y | ACS Appl. Mater. Interfaces 2015, 7, 791−800

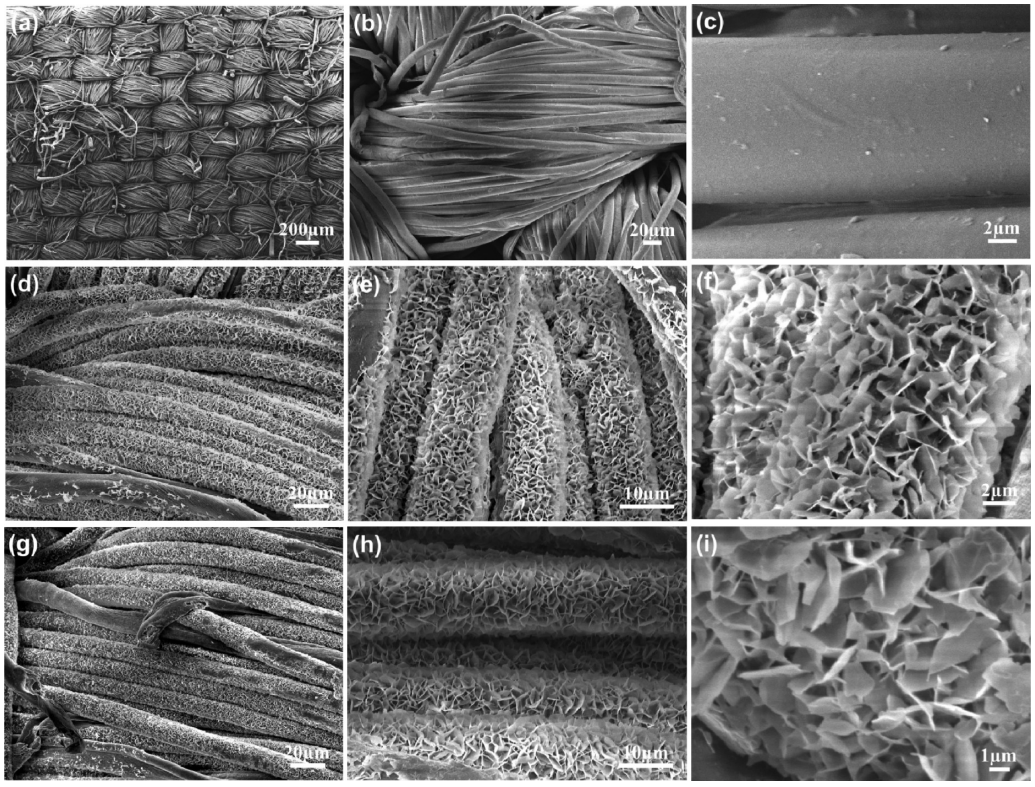

Figure 1. SEM images of the textiles with different magnification: (a–c) pristine textile; and (d–f) LDH coated sample before and (g–i) after the modification with sodium laurate.

deioinized water and dried in an oven at 60 °C. Finally, the LDH coated textile was immersed in a 0.02 M aqueous solution of sodium laurate at room temperature for 1 h. The resulting textile was rinsed with water and ethanol and then dried at room temperature.

Oil/Water Separation. Six kinds of oils and organic solvents including gasoline, diesel oil, *n*-hexane, chloroform, petroleum ether, and toluene were used in this study. They were colored with oil red O and mixed with water that was colored with methylene blue. The volume ratio of oil to water was varied at 1:1, 1:4, 1:9, 1:12, and 1:15. For oil/water separation, the superhydrophobic and superoleophilic textile was used as the membrane, and the mixtures of oil and water (or seawater) were poured slowly into a test tube through the textile. The separated oil and water were collected with a test tube and a beaker, respectively. The mass of the water before mixture and after separation was weighted to evaluate the separation efficiency, which was calculated according to $\eta = (m_1/m_0) \times 100\%$. Here, m_0 and m_1 were the mass of the water before and after the separation process, respectively. Additionally, another method was also used to show the separation efficiency qualitatively.[12] A mixture of oil and KCl aqueous solution was poured slowly into a test tube containing $AgNO_3$ solution through the as-prepared textile. Once there is a small amount of KCl aqueous solution penetrating the textile together with the oil, KCl will react with $AgNO_3$ to generate a white precipitate.

Removal of Oil from Water. A piece of the as-prepared textile or textile bag filled with sponge was placed into the oil/water mixtures (here, *n*-hexane and chloroform were used as the model oil and dyed red for clear observation) and then removed from the water surface by tweezer. The adsorbed oils were collected through a simple squeezing process. After each separation process, the textile or bag was washed with ethanol three times and dried for reusing.

Characterization. Scanning electron microscope (SEM) images were taken using a JEOL-7500F field-emission scanning electron microscope. Energy-dispersive X-ray spectra (EDX) were collected on the JEOL-7500F equipped with an EDAX detector. XRD data were measured on a D8 ADVANCE/Bruker AXS X-ray diffractometer with a Cu Kα X-ray radiation source. The water contact angle tests were performed on a DSA30 contact-angle system (Kruss, Germany) at room temperature. Transmission electron microscopy (TEM) images were obtained using a HITACHI HT7700 transmission electron microscope. The inductively coupled plasma optical emission spectroscopy (ICP-OES) was measured by using a PerkinElmer ICP Optima 800. Fourier transform infrared (FTIR) spectra were recorded by using Thermo Scientific Nicolet IR200 spectrometer. UV–visible absorption spectra were carried out by using a Persee TU-1901 UV–vis spectrometer.

3. RESULTS AND DISCUSSION

Growth of LDH Microcrystals on the Surface of Textile. The MgAl-LDH coated textile was obtained by using a method that involves separated nucleation and crystal growth steps. First, LDH seeds were prepared through a rapid coprecipitation process and then separated from the mother liquor. Second, commercial textile was immersed into the redispersed LDH seeds solution, and LDH coatings were developed at a crystal growth stage under hydrothermal conditions. It has been demonstrated that this simple hydrothermal process is able to fabricate LDH coatings of high quality as well as controllable pore size on various substrates including metal, ceramics, and glass of planar and nonplanar surfaces.[30] By using this process, LDH microcrystals were successfully in situ formed on the surface of textile as illustrated by scanning electron microscope (SEM) images (Figure 1). Obviously, the pristine textile has a macroscopically rough surface (Figure 1a) because it is made up of numerous microfibers with diameters ranging from 10 to 15 μm (Figure 1b). However, it is worth noting that these microfibers exhibit smooth surfaces at high magnification (Figure 1c). As compared to the pristine textile, the LDH coated textile not only displays roughness at macroscopy inherent from the

dx.doi.org/10.1021/am507238y | ACS Appl. Mater. Interfaces 2015, 7, 791–800

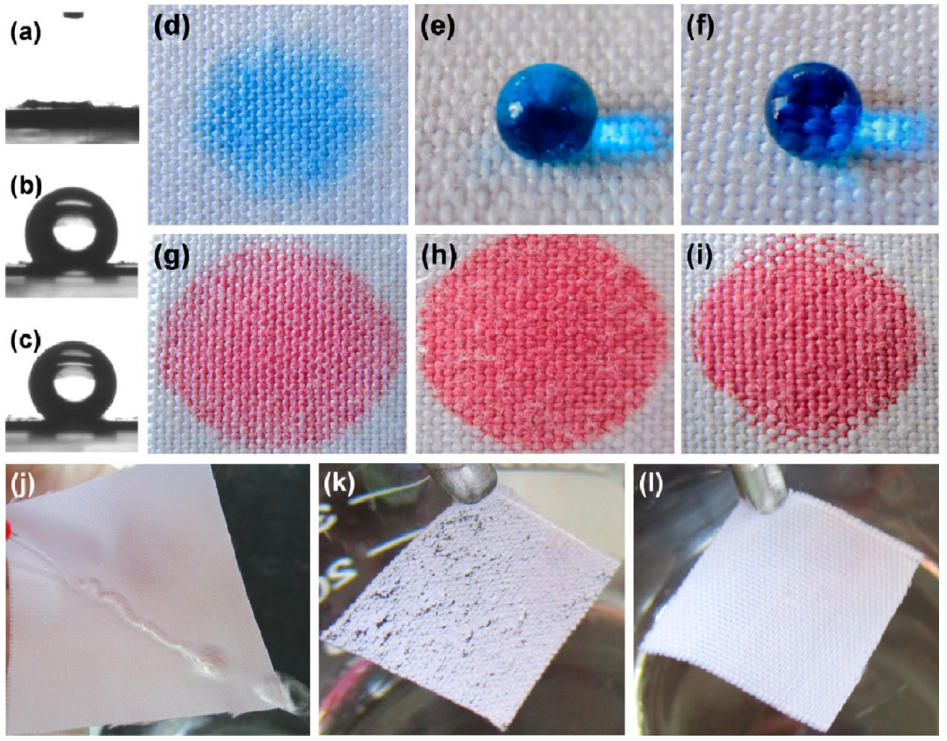

Figure 2. (a–c) Water contact angle (a) of pristine textile, (b) of LDH coated textile before, and (c) after the modification with sodium laurate; (d–i) photographs of (d–f) water and (g–i) oil placed on the surface of the above three kinds of textiles, respectively; (j) a jet of water applied on the as-prepared textile; (k) pristine textile in water; and (l) the as-prepared textile immersed in water by an external force.

microfibers (Figure 1d), but also shows roughness at the micro-/nanoscale due to the in situ formed LDH microcrystals. The morphology of the LDH microcrystals collected from the suspension of the same bath after hydrothermal reaction has been confirmed by transmission electron microscopy (TEM) images, which clearly illustrate the hexagonal plate-like structure of the LDH microcrystals (see Figure S1 in the Supporting Information). Furthermore, the LDH microcrystals with typical plate-like morphology stand vertically on the surface of microfibers, as shown in Figure 1e,f. They are densely packed and randomly oriented, generating a nestlike microstructure and producing large amounts of micrometer-sized and nanometer-sized spaces between LDH microcrystals. This feature is supposed to entrap numerous air pockets on the surface of microfibers, as demonstrated below. As is well-known, air pockets are necessary to achieve surface superhydrophobicity, because air is an effective hydrophobic medium. In addition to the hierarchical micro-/nanostructure of the surface, the hydrophobicity of the surface is also influenced by the surface free energy.[52−54] Thus, the LDH coated textile was further modified with sodium laurate to reduce the surface energy. The SEM images of the LDH coated textile after the modification with sodium laurate display no obvious changes in morphology (Figure 1g–i), confirming that the mild reaction does not damage the original microstructure and morphology of the LDH microcrystals.

The growth of LDH microcrystals on the surface of textile was further proved by the representative energy-dispersive X-ray spectrometry (EDS), inductively coupled plasma optical emission spectroscopy (ICP-OES), and X-ray diffraction (XRD). The EDS spectra taken on these samples reveal that the commercial textile mainly consists of carbon (66.32%, relative atomic % by element) and oxygen (31.03%) elements (see Figure S2a in the Supporting Information), while the LDH coated textile contains the elements magnesium and aluminum, apart from the initial carbon (43.50%) and oxygen (49.13%) (see Figure S2b in the Supporting Information). The existence of magnesium and aluminum is attributed to the immobilized LDH microcrystals. The atomic ratio of metal contents (Mg/Al) measured by ICP-OES is 2.1:1, coinciding with that in the precursor solution, and it is considered to be within the allowable experimental error range. Additionally, the decrease in the atomic ratio of the contents (C/O) originates from the high component of O contained in LDH microcrystals. These results clearly indicate that LDH microcrystals have been successfully formed on the surface of the textile. The modification with sodium laurate is confirmed by the increase of the atomic ratio of the contents (C/O), because of the high component of C element contained in sodium laurate (see Figure S2c in the Supporting Information). In all of these samples, the signal of Au element comes from the gold spray. Besides, the XRD patterns of the textile before (curve b) and after (curve c) MgAl-LDH coating, as well as LDH powder collected from the suspension of the same bath after hydrothermal reaction (curve a), are shown in Figure S3 in the Supporting Information. Although most of the LDH peaks overlap with those of the textile, an extra diffraction peak appears at the position indicated by the asterisk, which can be assigned to the (111) plane of the LDH crystals. These results provide evidence for the incorporation of MgAl-LDH on the textile.

Additionally, the ability of modification LDH with sodium laurate was verified by Fourier transform infrared (FTIR) spectra. As shown in Figure S4 in the Supporting Information, apart from the LDH feature peaks at 3471, 1558, and 1385 cm^{-1}, two characteristic peaks at 2926 and 2855 cm^{-1} have

been observed from the sodium laurate modified LDH sample. These two peaks are attributed to the asymmetric and symmetric C−H stretching bands of the long-chain aliphatic groups of laurate, indicating that LDH can be modified by sodium laurate. Furthermore, the effect of sodium laurate concentration on the hydrophobicity of the textile was optimized (see Figure S5 in the Supporting Information). As the concentration of sodium laurate increased, the water contact angle increased gradually until 0.02 M sodium laurate was used (see Figure S5(a) in the Supporting Information). The modification time is another factor that affects the hydrophobicity of the textile. As shown in Figure S5(b) in the Supporting Information, the water contact angle increased slowly when the modification time increased from 0 to 1 h. Afterward, little change was observed when further extending the immersing time. To obtain superhydrophobicity, the LDH-coated textile was modified with sodium laurate by immersing in 0.02 M sodium laurate solution for 1 h. As is well-known, the superhydrophobicity actually arises from the hierarchical micro-/nanostructure of the surface together with the low surface energy of the materials.[55−57] Therefore, the as-prepared textile is anticipated to have a hydrophobic surface.

Separation of Oil/Water Mixture. To verify the wetting behavior, water contact angle was measured, as shown in Figure 2a−c. For the pristine textile, when water was dropped on it, no contact angle could be observed due to the complete speading of water into the textile (Figure 2a,d). After coating the textile with LDH, it changed to be hydrophobic with a water contact angle of about 144 ± 1.2° (Figure 2b), whereas superhydrophobicity was achieved by further modification of the textile with sodium laurate, and its contact angle was found to be about 154 ± 1.6° (Figure 2c). These results implied that both the microstructure induced by LDH and the low surface energy of sodium laurate have significant contributions to the superhydrophobicity of the textile. As is well-known, the surface tension of water is commonly much higher than that of oil. When the surface tension of the solid substrate lies between those of water and oil, hydrophobicity and oleophilicity can be realized. Hence, a water droplet could sit on the surface of the functionalized textile as shown in Figure 2e,f. By contrast, oils with low surface tension can spread quickly on all of these textiles, indicating the superoleophilicity of these samples (Figure 2g−i). Furthermore, when a jet of water was applied on the as-prepared textile, it would roll off quickly without leaving a trace due to the existence of the air cushion between water and the textile (Figure 2j). The air cushion was further revealed by the bright and reflective surface observed beneath the water in Figure 2k. Obviously, most of the area underneath water was the liquid/air interface, and the ratio of liquid/solid interface was quite small. The establishment of a composite solid−liquid−air interface indicated the formation of the Cassie−Baxter state.[5] Moreover, the relationship between the surface structure and the surface contact angle can be explained by the Cassie−Baxter eq 1:[5]

$$\cos \theta_r = f_1 \cos \theta - f_2 \quad (1)$$

where θ_r and θ represent the contact angle of a rough surface and a native flat surface, while the f_1 and f_2 are the fraction areas of a liquid droplet in contact with surface and air on the surface, respectively ($f_1 + f_2 = 1$). According to the equation, the apparent contact angle increases with larger surface coverage and roughness of the micro-/nanostructure because of its higher f_2 value. Previous works have demonstrated that the formation of hierarchical structures can effectively enhance the surface roughness of the textile microfibers and hence increase the water contact angles on these surfaces.[8−11] On the basis of the established theory and experimental results, it is believed that surface roughness plays an important role on superhydrophobic surfaces, regardless of the chemical composition.[11] Therefore, although the LDH microcrystals are hydrophilic (see Figure S6 in the Supporting Information), the textile modified with LDH still exhibits hydrophobicity, because LDH crystals stand almost perpendicular to the surface of textile fibers, which largely increases the surface roughness. Thus, the observed superhydrophobicity of the functionalized textile is mainly attributed to the surface roughness induced by the nestlike LDH microstructures, which is favorable to trapping a large amount of air in voids and thus generates the hydrophobic surface. Besides, the hydrophobicity of the textile can be further increased by modification of the LDH with sodium laurate, which is reported to easily self-assemble onto the surface of LDH and decrease the surface free energy.[58] The possible reason is that the laurate anions can adsorb on the surface of LDH plates through electrostatic interaction with the hydrophilic heads pointing toward the cationic layers and the hydrophobic organic tails pointing outward, thus rendering the textile to be superhydrophobic.[58] As a result, the LDH and sodium laurate functionalized textile exhibit superhydrophobicity, which can trap air to form an air cushion under water and remain completely dry after the textile was taken out of water. As a comparison, no air cushion was observed for pristine textile, and its surface was not dry anymore (Figure 2l). In addition to the commercial plain weave polyester textile used above, similar results were also observed by using two other cotton textiles with different weaves as substrates (see Figures S7, S8 in the Supporting Information). As compared to the pristine textiles, the treated textiles have a superhydrophobic surface that cannot be wetted by water. Thus, the superhydrophobic textile cannot be penetrated by water, while the oil with low surface tension can easily pass through it. These properties endow the treated textiles to be a very promising candidate for separation of oil and water mixture.

The practical oil/water separation experiments were carried out by using a commercial plain weave polyester textile as a model. As shown in Figure 3a,b, when pouring the mixture of oil and water onto the treated textile, oil could pass through the textile rapidly and drop into the test tube beneath it, while water was retained on the surface of the textile and then flowed into another beaker. During the separation, no external force was used except their own weight. After the separation, no water in the collected oil or oil in the collected water can be seen. To further illustrate the absence of water in the collected oil, another simple experiment was performed, in which a mixture of oil and KCl aqueous solution was poured onto the textile and the penetrated oil was collected in a test tube containing $AgNO_3$ aqueous solution. As shown in Figure 3b, the $AgNO_3$ aqueous solution remained clear after the oil/water separation, whereas a white precipitate was generated quickly after adding a drop of KCl solution into the same solution (Figure 3c). This result implied that the coated textile could separate oil/water mixtures with high separation efficiency by a simple filtering method.

The separation efficiency of the textile was further investigated. Because oil is volatile and the textile will inevitably adsorb a part of oil, thus the separation efficiency was given by the ratio of the weight of water collected to that initially added

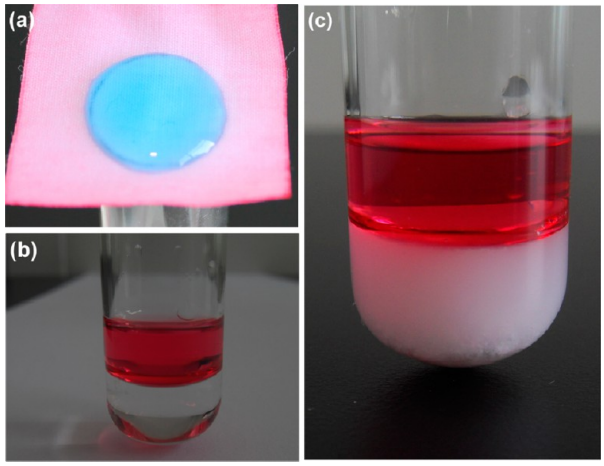

Figure 3. Photographs of (a) the separation of oil and water mixture, (b) collected oil in a test tube containing $AgNO_3$ aqueous solution, and (c) after adding a drop of KCl aqueous solution into (b). Oil was labeled with oil red O and KCl aqueous solution was labeled with methylene blue for easy observation.

to the mixture.[8] Table 1 lists the separation efficiency of the textile for different oil/water mixtures with their volume ratio of 1:1. Remarkably, the separation efficiency of the textile for the six oil/water mixtures was above 97%, and their relative standard deviation (RSD) values of five measurements were below 0.7%. It should be noted that the separation efficiency of the LDH-coated textile (95%) was slightly lower than that of the LDH-coated textile after modification with sodium laurate, possibly due to the small increase of the hydrophobicity induced by sodium laurate. Moreover, Table 2 indicated that the separation efficiency was calculated up to 98% for diesel oil/water mixtures with their volume ratios ranging from 1:1 to 1:15. The high separation efficiency is comparable with other similar superhydrophobic and superoleophilic materials.[8,15]

Table 1. Separation Efficiency of the Textile for Different Oil/Water Mixtures with Their Volume Ratios of 1:1 and Their Relative Standard Deviations (RSD) of Five Measurements

oil/water mixtures (volume ratio = 1:1)	separation efficiency (η, wt %)	relative standard deviations (RSD, %)
n-hexane/water	97.19	0.67
chloroform/water	97.60	0.64
toluene/water	98.31	0.35
petroleum ether/water	97.12	0.51
diesel oil/water	98.39	0.67
gasoline/water	98.01	0.48

Table 2. Separation Efficiency of the Textile for Diesel Oil/Water Mixtures with Different Volume Ratios and Their Relative Standard Deviations (RSD) of Five Measurements

diesel oil:water volume ratio	separation efficiency (η, wt %)	relative standard deviations (RSD %)
1:1	98.39	0.67
1:4	98.41	0.27
1:9	98.47	0.34
1:12	98.72	0.36
1:15	98.63	0.35

Besides, a high-quality oil/water separation material should be able to separate oil/seawater mixtures, because many oil leakages and spills occur in the ocean. Therefore, the as-prepared textile was employed to separate the mixture of oil/seawater by the simple filtering process. As shown in Figure 4,

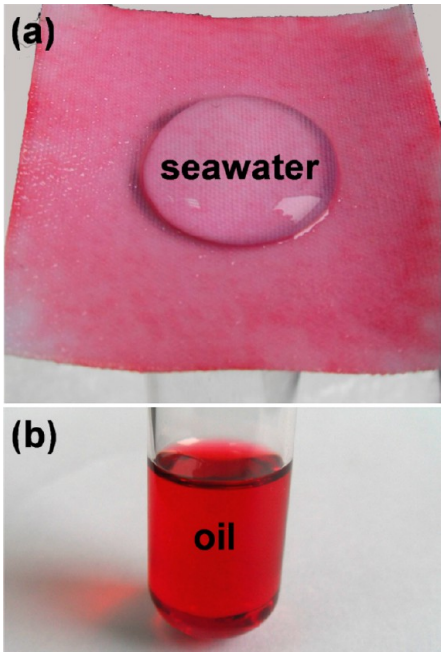

Figure 4. Photographs of (a) the separation of oil and seawater mixture and (b) collected oil in a test tube.

only oil could pass through the textile, and the seawater stayed on the surface of the textile. Hence, our superhydrophobic and superoleophilic textile could be utilized as filter membranes to realize highly effective separation of oil/water and oil/seawater mixtures.

Selective Adsorption of Oil. As mentioned above, the textile can separate oil/water mixtures with high efficiency. However, it is still unfeasible to separate a large amount of oil/water mixture arising from oil spills and other industrial organic pollutants, because it is unpractical to pour all of the mixtures onto the textile. Therefore, for practical application, the only way is to selectively adsorb oil and organic pollutants by immersing the adsorbent in the mixture.[59−68] In this respect, textile is an excellent candidate for preparing adsorbent materials due to their excellent properties, such as good flexibility, low price and density, as well as mechanical stability. As an example, a piece of superhydrophobic and superoleophilic textile fabricated in this study was used for separating oil from water (see movie S1 in the Supporting Information). When the textile was immersed into water, it strongly repelled water and remained dry after being taken out. However, when there was a layer of oil on the water surface, the superhydrophobic and superoleophilic textile quickly and selectively adsorbed the oil as soon as it touched the oil surface. Nevertheless, the application of this superhydrophobic and superoleophilic textile for the adsorption of oil from water was restricted by the inherent poor uptake capacity of textile. To circumvent this problem, the textile was made into a bag and filled with sponge. The filled bag was supposed to be an effective adsorbent for the removal of oil from water due to the combined advantages of the textile's superhydrophobicity,

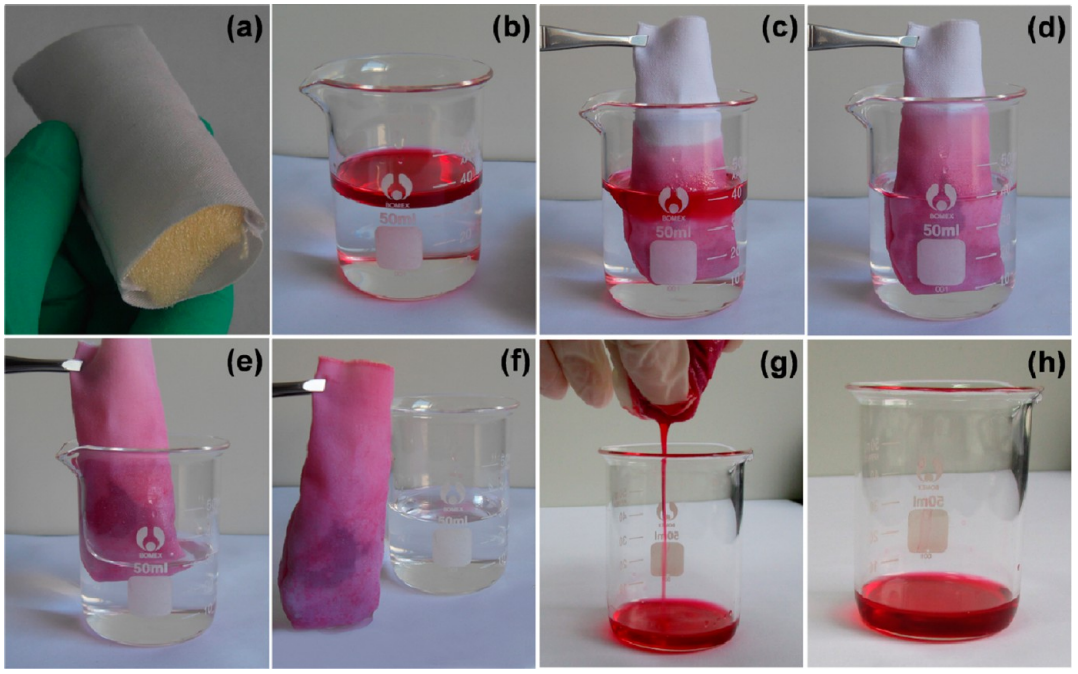

Figure 5. Photographs of (a) the textile bag, and (b–g) the oil adsorption and recycling process by using the superhydrophobic textile bag.

superoleophilicity, and the sponge's high porosity, in which the textile acted as a film for the selective separation of oil from water and the sponge acted as a container for storing the penetrated oil. The process of selective oil adsorption was shown in a series of photos in Figure 5a–f. By dipping the bag into a mixture of oil and water, the oil was quickly adsorbed and almost completely drawn out by the bag, leaving a fresh water surface. Importantly, the adsorbed oil can be collected by a manual squeezing process (Figure 5g,h). Although most of the adsorbed oil was squeezed out, there was still some residual oil sticking to the bag. So the bag was rinsed thoroughly by ethanol to remove the adsorbed oil and then dried in an oven at 50 °C. After drying, the superhydrophobicity of the bag could be recovered, and the bag could be reused as before. This adsorption and recovery process could be repeated at least 20 times without obvious change of the contact angle, as evidenced by Figure 6.

In the recovery process, ethanol was selected as eluent because of its advantages of nontoxicity, cost-effectiveness, and ability to dissolve most of the organic solvents and oils. To investigate the elution effect, *n*-hexane was used as model oil and colored with 10^{-3} M oil red O. After adsorption of oil, the textile was rinsed by immersing in 4 mL of ethanol to dissolve the adsorbed oil. Figure S9(a) in the Supporting Information shows that the absorption band of ethanol solution containing the eluted oil marked by oil red O was almost unchanged after 1 min. The results suggest that the equilibrium can be achieved within 1 min. Furthermore, no absorption band has been observed after rinsing three times (see Figure S9(b) in the Supporting Information), implying the complete removal of the organic oil. The excellent elution effect is possibly due to the high dissolution ability of ethanol to other organic solvents and oils.

To further verify the feasibility for practical application, the adsorption of chloroform from water was carried out to investigate the oil/water separation performance of the bag for the organic solvent that had higher density than water (see movie S2 in the Supporting Information). Once the bag was inserted into the oil/water surface, the dyed chloroform was immediately sucked up by the bag underwater and removed by taking out the bag. This process happened in less than 1 min, indicating the fast adsorption kinetics of the bag, which may be attributed to the combination of its oleophilic nature and capillary action. As compared to other materials for adsorption of oil from water, the reported process was simple, time-saving, and inexpensive. Therefore, the bag is an attractive candidate material for the application of oil spill cleanup and industrial oily wastewater treatment.

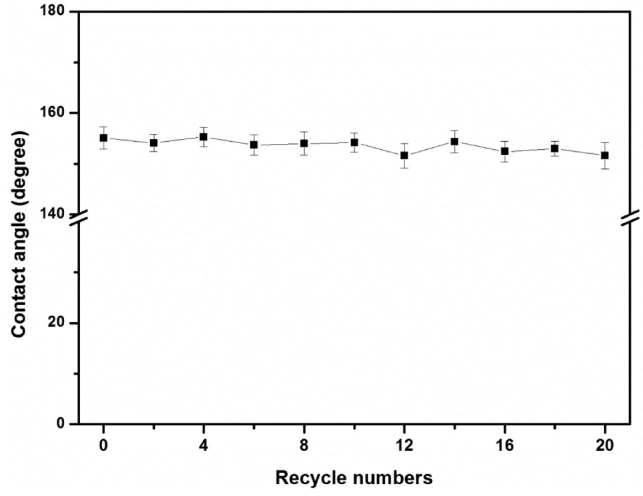

Figure 6. Water contact angles recorded after each oil/water separation process.

4. CONCLUSIONS

In summary, commercial textile was coated with LDH microcrystals through a simple and facile hydrothermal approach and then modified with sodium laurate. The unique nestlike microstructures induced by the in situ formed LDH

microcrystals and the modification of low surface energy chemical made the textile superhydrophobic and superoleophilic. Further experiments demonstrated that the as-obtained textile can effectively separate both light oil (density lower than that of water) and heavy oil (density greater than that of water) with high separation efficiency, which is up to 97%. Moreover, the bag prepared by the textile exhibited excellent selective oil adsorption capacity and reusability. Thus, this superhydrophobic and superoleophilic textile may find a wide range of practical applications such as in the cleanup of marine oil spills, recovery, and fuel purification.

■ ASSOCIATED CONTENT

Supporting Information

TEM images of the LDH microcrystals; EDS spectra of textile before and after functionalization of LDH and sodium laurate; XRD patterns of LDH powder, pristine textile, and LDH coated textile; FTIR spectra of Mg−Al LDH before and after medication with sodium laurate; water contact angles of LDH-coated textile after immersing in different concentrations of sodium laurate solution and immersing for different time; water contact angle of LDH crystals drop-casted on glass plate; water contact angles and wetting abilities of two cotton textiles before and after functionalization; UV−vis spectra of the ethanol solvent in the elution step; and movies of oil adsorption process by using textile and textile bag. This material is available free of charge via the Internet at http://pubs.acs.org.

■ AUTHOR INFORMATION

Corresponding Author

*Tel.: 86-532-86080855. Fax: 86-532-86080855. E-mail: lifeng@qust.edu.cn.

Notes

The authors declare no competing financial interest.

■ ACKNOWLEDGMENTS

This work was financially supported by the National Natural Science Foundation of China (nos. 21405089, 21375072, and 21175076), Scientific Research Award Fund for Excellent Middle-aged and Young Scientists of Shandong Province (no. BS2013DX025), and the Research Foundation for Distinguished Scholars of Qingdao Agricultural University (nos. 631311 and 631404).

■ REFERENCES

(1) Dalton, T.; Jin, D. Extent and Frequency of Vessel Oil Spills in US Marine Protected Areas. *Mar. Pollut. Bull.* **2010**, *60*, 1939−1945.
(2) Toyoda, M.; Inagaki, M. Sorption and Recovery of Heavy Oils by Using Exfoliated Graphite. *Spill Sci. Technol. Bull.* **2007**, *8*, 467−474.
(3) Yuan, J. K.; Liu, X. G.; Akbulut, O.; Hu, J. Q.; Suib, S. L.; Kong, J.; Stellacci, F. Superwetting Nanowire Membranes for Selective Absorption. *Nat. Nanotechnol.* **2008**, *3*, 332−336.
(4) Wenzel, R. W. Resistance of Solid Surfaces to Wetting by Water. *Ind. Eng. Chem.* **1936**, *28*, 988−994.
(5) Cassie, A. B. D.; Baxter, S. Wettability of Porous Surfaces. *Trans. Faraday Soc.* **1944**, *40*, 546−551.
(6) Feng, X. J.; Jiang, L. Design and Creation of Superwetting/Antiwetting Surfaces. *Adv. Mater.* **2006**, *18*, 3063−3078.
(7) Liu, M. J.; Jiang, L. Switchable Adhesion on Liquid/Solid Interfaces. *Adv. Funct. Mater.* **2010**, *20*, 3753−3764.
(8) Pan, Q. M.; Wang, M.; Wang, H. B. Separating Small Amount of Water and Hydrophobic Solvents by Novel Superhydrophobic Copper Meshes. *Appl. Surf. Sci.* **2008**, *254*, 6002−6006.
(9) Wang, C. X.; Yao, T. J.; Wu, J.; Ma, C.; Fan, Z. X.; Wang, Z. Y.; Cheng, Y. R.; Lin, Q.; Yang, B. Facile Approach in Fabricating Superhydrophobic and Superoleophilic Surface for Water and Oil Mixture Separation. *ACS Appl. Mater. Interfaces* **2009**, *1*, 2613−2617.
(10) Wang, B.; Li, J.; Wang, G. Y.; Liang, W. X.; Zhang, Y. B.; Shi, L.; Guo, Z. G.; Liu, W. M. Methodology for Robust Superhydrophobic Fabrics and Sponges from In Situ Growth of Transition Metal/Metal Oxide Nanocrystals with Thiol Modification and Their Applications in Oil/Water Separation. *ACS Appl. Mater. Interfaces* **2013**, *5*, 1827−1839.
(11) Ling, W. X.; Guo, Z. G. Stable Superhydrophobic and Superoleophilic Soft Porous Materials for Oil/Water Separation. *RSC Adv.* **2013**, *3*, 16469−16474.
(12) Zhang, J.; Seeger, S. Polyester Materials with Superwetting Silicone Nanofilaments for Oil/Water Separation and Selective Oil Absorption. *Adv. Funct. Mater.* **2011**, *21*, 4699−4704.
(13) Zhou, H.; Wang, H. X.; Niu, H. T.; Gestos, A.; Wang, X. G.; Lin, T. Fluoroalkyl Silane Modified Silicone Rubber/Nanoparticle Composite: A Super Durable, Robust Superhydrophobic Fabric Coating. *Adv. Mater.* **2012**, *24*, 2409−2412.
(14) Zhou, X. Y.; Zhang, Z. Z.; Xu, X. H.; Guo, F.; Zhu, X. T.; Men, X. H.; Ge, B. Robust and Durable Superhydrophobic Cotton Fabrics for Oil/Water Separation. *ACS Appl. Mater. Interfaces* **2013**, *5*, 7208−7214.
(15) Wang, S. H.; Li, M.; Lu, Q. H. Filter Paper with Selective Absorption and Separation of Liquids that Differ in Surface Tension. *ACS Appl. Mater. Interfaces* **2010**, *3*, 677−683.
(16) Zhuo, L. H.; Ge, J. C.; Cao, L. H.; Tang, B. Solvothermal Synthesis of CoO, Co_3O_4, $Ni(OH)_2$ and $Mg(OH)_2$ Nanotubes. *Cryst. Growth Des.* **2009**, *9*, 1−6.
(17) Liu, X. J.; Zong, C. H.; Ai, K. L.; He, W. H.; Lu, L. H. Engineering Natural Materials as Surface-Enhanced Raman Spectroscopy Substrates for In situ Molecular Sensing. *ACS Appl. Mater. Interfaces* **2012**, *4*, 6599−6608.
(18) Ma, R. Z.; Liu, Z. P.; Li, L.; Iyi, N.; Sasaki, T. Exfoliating Layered Double Hydroxides in Formamide: A Method to Obtain Positively Charged Nanosheets. *J. Mater. Chem.* **2006**, *16*, 3809−3813.
(19) Wang, Q.; O'Hare, D. Recent Advances in the Synthesis and Application of Layered Double Hydroxide (LDH) Nanosheets. *Chem. Rev.* **2012**, *112*, 4121−4155.
(20) Chen, D.; Wang, X. Y.; Liu, T. X.; Wang, X. D.; Li, J. Electrically Conductive Poly(vinyl alcohol) Hybrid Films Containing Graphene and Layered Double Hydroxide Fabricated via Layer-by-Layer Self-Assembly. *ACS Appl. Mater. Interfaces* **2010**, *2*, 2005−2011.
(21) Wen, T.; Wu, X. L.; Tan, X. L.; Wang, X. K.; Xu, A. W. One-Pot Synthesis of Water-Swellable Mg−Al Layered Double Hydroxides and Graphene Oxide Nanocomposites for Efficient Removal of As(V) from Aqueous Solutions. *ACS Appl. Mater. Interfaces* **2013**, *5*, 3304−3311.
(22) Teramura, K.; Iguchi, S. J.; Mizuno, Y.; Shishido, T.; Tanaka, T. Photocatalytic Conversion of CO_2 in Water over Layered Double Hydroxides. *Angew. Chem., Int. Ed.* **2012**, *51*, 8008−8011.
(23) Zhao, Y. F.; Li, B.; Wang, Q.; Gao, W.; Wang, C. J.; Wei, M.; Evans, D. G.; Duan, X.; O'Hare, D. NiTi-Layered Double Hydroxides Nanosheets as Efficient Photocatalysts for Oxygen Evolution from Water Using Visible Light. *Chem. Sci.* **2014**, *5*, 951−958.
(24) Shao, M. F.; Ning, F. Y.; Zhao, J. W.; Wei, M.; Evans, D. G.; Duan, X. Preparation of Fe_3O_4@SiO_2@Layered Double Hydroxide Core−Shell Microspheres for Magnetic Separation of Proteins. *J. Am. Chem. Soc.* **2012**, *134*, 1071−1077.
(25) Chen, C. P.; Gunawan, P.; Xu, R. Self-Assembled Fe_3O_4-Layered Double Hydroxide Colloidal Nanohybrids with Excellent Performance for Treatment of Organic Dyes in Water. *J. Mater. Chem.* **2011**, *21*, 1218−1225.
(26) Wang, H. T.; Ma, H. Y.; Zheng, W.; An, D. D.; Na, C. Z. Multifunctional and Recollectable Carbon Nanotube Ponytails for Water Purification. *ACS Appl. Mater. Interfaces* **2014**, *6*, 9426−9434.
(27) Han, J. B.; Dou, Y. B.; Wei, M.; Evans, D. G.; Duan, X. Erasable Nanoporous Antireflection Coatings Based on the Reconstruction

Effect of Layered Double Hydroxides. *Angew. Chem., Int. Ed.* **2010**, *49*, 2171−2174.
(28) Gu, Z.; Thomas, A. C.; Xu, Z. P.; Campbell, J. H.; Lu, G. Q. In Vitro Sustained Release of LMWH from MgAl-Layered Double Hydroxide Nanohybrids. *Chem. Mater.* **2008**, *20*, 3715−3722.
(29) Gunawan, P.; Xu, R. Direct Assembly of Anisotropic Layered Double Hydroxide (LDH) Nanocrystals on Spherical Template for Fabrication of Drug-LDH Hollow Nanospheres. *Chem. Mater.* **2009**, *21*, 781−783.
(30) Chen, C. P.; Gunawan, P.; Lou, X. W.; Xu, R. Silver Nanoparticles Deposited Layered Double Hydroxide Nanoporous Coatings with Excellent Antimicrobial Activities. *Adv. Funct. Mater.* **2011**, *22*, 780−787.
(31) Chen, H. Y.; Zhang, F. Z.; Fu, S. S.; Duan, X. In Situ Microstructure Control of Oriented Layered Double Hydroxide Monolayer Films with Curved Hexagonal Crystals as Superhydrophobic Materials. *Adv. Mater.* **2006**, *18*, 3089−3093.
(32) You, Y. W.; Zhao, H. T.; Vance, G. F. Hybrid Organic−Inorganic Derivatives of Layered Double Hydroxides and Dodecylbenzenesulfonate: Preparation and Adsorption Characteristics. *J. Mater. Chem.* **2002**, *12*, 907−912.
(33) Zhang, F. Z.; Zhao, L. L.; Chen, H. Y.; Xu, S. L.; Evans, D. G.; Duan, X. Corrosion Resistance of Superhydrophobic Layered Double Hydroxide Films on Aluminum. *Angew. Chem., Int. Ed.* **2008**, *47*, 2466−2469.
(34) Dutta, K.; Pramanik, A. Synthesis of A Novel Cone-Shaped CaAl-layered Double Hydroxide (LDH): Its Potential Use as A Reversible Oil Sorbent. *Chem. Commun.* **2013**, *49*, 6427−6429.
(35) Li, L.; Ma, R. Z.; Ebina, Y.; Iyi, N.; Sasaki, T. Positively Charged Nanosheets Derived via Total Delamination of Layered Double Hydroxides. *Chem. Mater.* **2005**, *17*, 4386−4391.
(36) Lee, J. H.; Rhee, S. W.; Jung, D. Y. Selective Layer Reaction of Layer-by-Layer Assembled Layered Double-Hydroxide Nanocrystals. *J. Am. Chem. Soc.* **2007**, *129*, 3522−3523.
(37) Okamoto, K.; Sasaki, T.; Fujita, T.; Iyi, N. Preparation of Highly Oriented Organic−LDH Hybrid Films by Combining the Decarbonation, Anion-Exchange, and Delamination Processes. *J. Mater. Chem.* **2006**, *16*, 1608−1616.
(38) Wang, Q.; Zhang, X.; Zhu, J. H.; Guo, Z. H.; O'Hare, D. Preparation of Stable Dispersions of Layered Double Hydroxides (LDHs) in Nonpolar Hydrocarbons: New Routes to Polyolefin/LDH Nanocomposites. *Chem. Commun.* **2012**, *48*, 7450−7452.
(39) Lee, J. H.; Rhee, S. W.; Jung, D. Y. Solvothermal Ion Exchange of Aliphatic Dicarboxylates into the Gallery Space of Layered Double Hydroxides Immobilized on Si Substrates. *Chem. Mater.* **2004**, *16*, 3774−3779.
(40) Lee, J. H.; Rhee, S. W.; Jung, D. Y. Orientation-Controlled Assembly and Solvothermal Ion-Exchange of Layered Double Hydroxide Nanocrystals. *Chem. Commun.* **2003**, 2740−2741.
(41) Dutta, K.; Das, S.; Pramanik, A. Concomitant Synthesis of Highly Crystalline Zn-Al Layered Double Hydroxide and ZnO: Phase Interconversion and Enhanced Photocataytis Activity. *J. Colloid Interface Sci.* **2012**, *366*, 28−36.
(42) Lin, M. C.; Chang, F. T.; Uan, J. Y. Synthesis of Li−Al−Carbonate Layered Double Hydroxide in A Metal Salt−Free System. *J. Mater. Chem.* **2010**, *20*, 6524−6530.
(43) Uan, J. Y.; Lin, J. K.; Tung, Y. S. Direct Growth of Oriented Mg−Al Layered Double Hydroxide Film on Mg Alloy in Aqueous HCO_3^-/CO_3^{2-} solution. *J. Mater. Chem.* **2010**, *20*, 761−766.
(44) Lü, Z.; Zhang, F. Z.; Lei, X. D.; Yang, L.; Xu, S. L.; Duan, X. In situ Growth of Layered Double Hydroxide Films on Anodic Aluminum Oxide/Aluminum and Its Catalytic Feature in Aldol Condensation of Acetone. *Chem. Eng. Sci.* **2008**, *63*, 4055−4062.
(45) Chen, H. Y.; Zhang, F. Z.; Chen, T.; Xu, S. L.; Evans, D. G.; Duan, X. Comparison of the Evolution and Growth Processes of Films of M/Al-Layered Double Hydroxides with M=Ni or Zn. *Chem. Eng. Sci.* **2009**, *64*, 2617−2622.
(46) Liu, J. P.; Li, Y. Y.; Huang, X. T.; Li, G. Y.; Li, Z. K. Layered Double Hydroxide Nano- and Microstructures Grown Directly on Metal Substrates and Their Calcined Products for Application as Li-Ion Battery Electrodes. *Adv. Funct. Mater.* **2008**, *18*, 1448−1458.
(47) Lü, Z.; Zhang, F. Z.; Lei, X. D.; Yang, L.; Evans, D. G.; Duan, X. Microstructure-Controlled Synthesis of Oriented Layered Double Hydroxide Thin Films: Effect of Varying the Preparation Conditions and A Kinetic and Mechanistic Study of Film Formation. *Chem. Eng. Sci.* **2007**, *62*, 6069−6057.
(48) Guo, X. X.; Zhang, F. Z.; Xu, S. L.; Evans, D. G.; Duan, X. Preparation of Layered Double Hydroxide Films with Different Orientations on the Opposite Sides of A Glass Substrate by In Situ Hydrothermal Crystallization. *Chem. Commun.* **2009**, 6836−6838.
(49) Zhao, Y. F.; He, S.; Wei, M.; Evans, D. G.; Duan, X. Hierarchical Films of Layered Double Hydroxides by Using A Sol−Gel Process and Their High Adaptability in Water Treatment. *Chem. Commun.* **2010**, *46*, 3031−3033.
(50) Hsieh, Z. L.; Lin, M. C.; Uan, J. Y. Rapid Direct Growth of Li−Al Layered Double Hydroxide (LDH) Film on Glass, Silicon Wafer and Carbon Cloth and Characterization of LDH Film on Substrates. *J. Mater. Chem.* **2011**, *21*, 1880−1889.
(51) Xu, Z. P.; Stevenson, G. S.; Lu, C. Q.; Lu, G. Q.; Bartlett, P. F.; Gray, P. P. Stable Suspension of Layered Double Hydroxide Nanoparticles in Aqueous Solution. *J. Am. Chem. Soc.* **2006**, *128*, 36−37.
(52) Boduroglu, S.; Cetinkaya, M.; Dressick, W. J.; Singh, A.; Demirel, M. C. Controlling the Wettability and Adhesion of Nanostructured Poly-(p-xylylene) Films. *Langmuir* **2007**, *23*, 11391−11395.
(53) Lai, Y. K.; Lin, C. J.; Huang, J. Y.; Zhuang, H. F.; Sun, L.; Nguyen, T. Markedly Controllable Adhesion of Superhydrophobic Spongelike Nanostructure TiO_2 Films. *Langmuir* **2008**, *24*, 3867−3873.
(54) Tian, D. L.; Zhang, X. F.; Wang, X.; Zhai, J.; Jiang, L. Micro/Nanoscale Hierarchical Structured ZnO Mesh Film for Separation of Water and Oil. *Phys. Chem. Chem. Phys.* **2011**, *13*, 14606−14610.
(55) Quéré, D.; Lafuma, A.; Bico, J. Slippy and Sticky Microtextured Solids. *Nanotechnology* **2003**, *14*, 1109−1112.
(56) Huang, X. J.; Kim, D. H.; Im, M.; Lee, J. H.; Yoon, J. B.; Choi, Y. K. Lock-and-Key" Geometry Effect of Patterned Surfaces: Wettability and Switching of Adhesive Force. *Small* **2009**, *5*, 90−94.
(57) Cao, Y. Z.; Zhang, X. Y.; Tao, L.; Li, K.; Xue, Z. X.; Feng, L.; Wei, Y. Mussel-Inspired Chemistry and Michael Addition Reaction for Efficient Oil/Water Separation. *ACS Appl. Mater. Interfaces* **2013**, *5*, 4438−4442.
(58) Fan, G. L.; Xiang, X.; Fan, J.; Li, F. Template-Assisted Fabrication of Macroporous $NiFe_2O_4$ Films with Tunable Microstructural, Magnetic and Interfacial Properties. *J. Mater. Chem.* **2010**, *20*, 7378−7385.
(59) Choi, H. M.; Cloud, R. M. Natural Sorbents in Oil Spill Cleanup. *Environ. Sci. Technol.* **1992**, *26*, 772−776.
(60) Zadaka-Amir, D.; Bleiman, N.; Mishael, Y. G. Sepiolite as An Effective Natural Porous Adsorbent for Surface Oil-Spill. *Microporous Mesoporous Mater.* **2013**, *169*, 153−159.
(61) Teli, M. D.; Valia, S. P. Acetylation of Banana Fibre to Improve Oil Absorbency. *Carbohydr. Polym.* **2013**, *92*, 328−333.
(62) Angelova, D.; Uzunov, I.; Uzunova, S.; Gigova, A.; Minchev, L. Kinetics of Oil and Oil Products Adsorption by Carbonized Rice Husks. *Chem. Eng. J.* **2011**, *172*, 306−311.
(63) Feng, L.; Zhang, Z. Y.; Mai, Z. H.; Ma, Y. M.; Liu, B. Q.; Jiang, L.; Zhu, D. B. A Super-Hydrophobic and Super-Oleophilic Coating Mesh Film for the Separation of Oil and Water. *Angew. Chem., Int. Ed.* **2004**, *43*, 2012−2014.
(64) Chu, Y.; Pan, Q. M. Three-Dimensionally Macroporous Fe/C Nanocomposites as Highly Selective Oil-Absorption Materials. *ACS Appl. Mater. Interfaces* **2012**, *4*, 2420−2425.
(65) Bi, H. C.; Xie, X.; Yin, K. B.; Zhou, Y. L.; Wan, S.; He, L. B.; Xu, F.; Banhart, F.; Sun, L. T.; Ruoff, R. S. Spongy Graphene as a Highly Efficient and Recyclable Sorbent for Oils and Organic Solvents. *Adv. Funct. Mater.* **2012**, *22*, 4421−4425.

(66) Wei, G.; Miao, Y. E.; Zhang, C.; Yang, Z.; Liu, Z. Y.; Tjiu, W. W.; Liu, T. X. Ni-Doped Graphene/Carbon Cryogels and Their Applications As Versatile Sorbents for Water Purification. *ACS Appl. Mater. Interfaces* **2013**, *5*, 7584−7591.
(67) Ruan, C. P.; Ai, K. L.; Li, X. B.; Lu, L. H. A Superhydrophobic Sponge with Excellent Absorbency and Flame Retardancy. *Angew. Chem., Int. Ed.* **2014**, *53*, 5556−5560.
(68) Tai, M. H.; Gao, P.; Tan, B. Y. L.; Sun, D. D.; Leckie, J. O. Highly Efficient and Flexible Electrospun Carbon−Silica Nanofibrous Membrane for Ultrafast Gravity−Driven Oil−Water Separation. *ACS Appl. Mater. Interfaces* **2014**, *6*, 9393−9401.